Published in final edited form as:
IEEE Trans Neural Syst Rehabil Eng. 2013 March ; 21(2): 319–328. doi:10.1109/TNSRE.2013.2245423.

Safe Direct Current Stimulation to Expand Capabilities of Neural Prostheses

Gene Y. Fridman [IEEE, Member] and
Department of Otolaryngology Head and Neck Surgery, Johns Hopkins University, Baltimore, MD 21208

Charles C. Della Santina [IEEE, Member]
Department of Otolaryngology Head and Neck Surgery, Johns Hopkins University, Baltimore, MD 21208

Department of Biomedical Engineering at the Johns Hopkins University

Abstract

While effective in treating some neurological disorders, neuroelectric prostheses are fundamentally limited because they must employ charge-balanced stimuli to avoid evolution of irreversible electrochemical reactions and their byproducts at the interface between metal electrodes and body fluids. Charge-balancing is typically achieved by using brief biphasic alternating current (AC) pulses, which typically excite nearby neural tissues but cannot efficiently inhibit them. In contrast, direct current (DC) applied via a metal electrode in contact with body fluids can excite, inhibit and modulate sensitivity of neurons; however, DC stimulation is biologically unsafe because it violates “safe charge injection” limits that have long been considered unavoidable constraints. In this report, we describe the design and fabrication of a safe DC stimulator (SDCS) that overcomes this constraint. The SCDS drives DC ionic current into target tissue via salt-bridge micropipette electrodes by switching valves in phase with AC square waves applied to metal electrodes contained within the device. This approach achieves DC ionic flow through tissue while still adhering to charge-balancing constraints at each electrode-saline interface. We show the SDCS’s ability to both inhibit and excite neural activity to achieve improved dynamic range during prosthetic stimulation of the vestibular part of the inner ear in chinchillas.

I.INTRODUCTION

Pacemakers, cochlear implants, and essentially all other chronically implanted neuroelectric prostheses used in clinical settings rely on charge-balanced, biphasic pulses or other forms of alternating current (AC) to excite neural or muscular activity without driving electrochemical reactions that would otherwise liberate toxic substances at the electrode-saline interface [1;2]. All of these devices are constrained to excite the neural tissue in which

Address correspondence to: Gene Y. Fridman PhD, Johns Hopkins Vestibular NeuroEngineering Lab 720 Rutland Ave, Suite 830, Baltimore MD 21205 gfridma1@jhmi.edu (818)389-0699.

The terms of these arrangements are being managed by the Johns Hopkins University in accordance with its conflict of interest policies.

they are implanted. Inhibition is difficult to achieve with these devices, because the need to avoid a net charge flow above a small "safe charge injection" threshold (e.g., ~100 μC/cm^2 electrode area for platinum electrodes [3–5]) mandates the use of brief, charge-balanced pulses for which the cathodic, excitatory phase dominates the neural response.

When the target neural tissue is spontaneously active and the therapeutic goal is to *inhibit* activity, AC neuroelectric prostheses such as deep brain stimulators (DBS) [6] and spinal cord stimulators (SCS) [7;8] typically work indirectly by exciting a set of neurons that then trans-synaptically inhibit the actual target or by driving a set of afferent neurons at supernormal rates to engender downstream adaptive changes that allow encoding of inhibition through withdrawal of excitation. Alternatively, high frequency pulse trains (1–30kHz) have been used to create nerve conduction block; however, broad application of that approach is constrained by the relatively high current required to achieve effective block and by the long (~10s) excitatory phase typically associated with the onset of stimulation [9–11].

A neural prosthesis that can both excite and inhibit neural tissue could dramatically improve treatment of many neurologic deficits. For example, prostheses to assist micturition should simultaneously excite sacral nerves to activate the detrusor muscle and inhibit lumbar nerves to relax the urethral sphincter [11]. Prostheses intended to restore balance and stable vision through action on the inner ear vestibular afferent fibers require not only excitation to encode head motion toward the implanted side of the head but also inhibition to encode head motion in the opposite direction [12]. Several highly prevalent disorders characterized by uncontrolled neural firing rates (such as tinnitus [13], chronic pain [14], and epilepsy [15]) could be effectively treated by implantable prostheses capable of neural inhibition.

Anodic *direct current* (DC) delivered by an extracellular electrode near target tissue is very effective at inhibiting neural activity, and continuous cathodic DC can excite neural activity in a graded, stochastic fashion unlike the deterministic, phase-locked behavior elicited by pulsatile stimuli. Given these advantages, DC has long been a mainstay of laboratory experiments, in which the charge-balance constraints imposed on chronically implanted medical devices can be ignored (at the expense of eventual electrode corrosion and neuronal death) or overcome through the use of electrodes that are very large or otherwise incompatible with chronic implantation. Unfortunately, DC stimulation protocols have not been available to implantable medical device designers during most of the 54 years since the first successful demonstration of a chronically implanted pacemaker [16].

An elegant solution to this dilemma was initially described as a method for treating sensorineural hearing loss by Spelman *et al.*, who created a switching network that effectively delivered DC ionic flow into target tissue by switching mechanical valves in phase with AC square waves applied to metal electrodes immersed in an ionic solution [17;18]. Based on this idea, we designed and built a Safe DC Stimulator (SDCS) prototype, the SDCS1. We demonstrate that the SDCS1 can both excite and inhibit neurons in chinchillas implanted with microcatheter salt bridge electrodes. We discuss further directions for technological improvements, necessary safety investigations, and potential applications of this technology.

II. Safe Direct Current Stimulator Prototype

A. Safe DC Concept

Conceptually, the SDCS delivers alternating current pulses to electrodes suspended at the opposite ends of a torus filled with ionic solution ("saline" in Fig.1). With each change in stimulation polarity, valves on either side of each electrode switch from open-to-closed or vice versa, effectively modulating the path for ionic flow through each valve between low impedance and high impedance. Two extension tubes connect the sides of the torus to body fluids to complete the ionic current circuit. Figure 1 demonstrates this concept and illustrates the two states of the apparatus. In both states, ionic current flows from left to right through the implanted tissue. In this way, a continuous AC square wave controlling the apparatus can deliver approximately DC ionic current through the tissue from left to right.

B. SDCS1 Prototype

To confirm that an SDCS can deliver ionic DC current as intended, we built and bench-tested a prototype of the SDCS, the SDCS1. Figure 2A shows the two states of the device corresponding to the states schematized in Figure 1. We used normally-closed valves (Model DDB-CD-12VDC, Ehcotech International Inc., San Diego, CA) interconnected with silicone surgical tubing filled with 0.9% NaCl aqueous solution. The valves were operated using the circuit on the bottom right of the diagrams in Figure 2A. A positive voltage from the stimulator source caused B valves to open and A valves to close (left part of the panel). Conversely, negative voltage caused A valves to open and B valves to close (right part of the panel). Valve operation was synchronized to electrode polarity changes because the valves were controlled by the square wave AC signal applied to the electrodes e_A and e_B.

To drive the current through the system we used two AM2100 biphasic isolated pulse stimulator systems (A–M Systems, Carlsborg, WA), which were synchronized to deliver 0.5 Hz biphasic pulses to the eA and eB metal electrodes and provided the control signal for the valve driver circuit. We used two AM2100's in series because the leakage current within the SDCS1 through the closed valves and the high output impedance of the system imposed by the narrow diameter tubes connecting the system to the tissue required >100V compliance voltage to achieve stimulation currents from ~0–250μA.

The output current of the SDCS can vary with the diameter of the tubes that conduct ionic current to the tissue, the impedance of the ionic fluid that fills the system, and leakage currents throughout the system. To monitor the output of the SDCS, we developed and calibrated a current sensing element (CSE) (Fig. 2B). This sensor is functionally analogous to a "sense resistor" used in electronic circuits. It is inserted in line at the system output to the tissue as shown in Figure 2A. The sensor is composed of two biocompatible stainless steel hollow tubes that serve as sensing electrodes at the opposite ends of a silicone tube filled with conductive gel. The conductive gel creates a salt bridge that allows the ions to flow through, but maintains the structural integrity and constant impedance of the CSE. The CSE conduction gel in our system was composed of 0.9% NaCl saline mixed with LB-Agar Medium (Q-Bio gene, Carlsbad, CA) at approximately 0.1 g/ml. The voltage between the

two sensing electrodes is proportional to the ionic current through the sensor. This voltage is measured differentially to monitor the output current of the system.

Stimulation current from the SDCS1 is delivered to the target tissue using ionic solution rather than metal wires (Fig. 2A,C). To deliver ionic current at high current density via small points of entry into the inner ear, we created a modified and miniaturized version of the separated interface nerve electrodes described by Ackerman et al. [19]. To prepare these tube electrodes (TE) we filled Eppendorf 20μL capillary tubes with a sterile mixture of agar and artificial perilymph [20] to mimic the ionic profile of the labyrinthine fluid. While the gel freely conducts the ionic current from the SDCS, it resists fluid motion in and out of the tube and it offers a physical barrier to biological contamination of the implanted tissue.

III. Methods

A. SDCS1 Bench Test

We calibrated the CSE using an AM2200 constant current source (A-M Systems, Carlsborg, WA) passing 0μA to 70μA via large metal electrodes (22 gauge stainless steel needles) through saline-filled surgical tubes connected to a saline bath via a CSE (Fig. 2B). We recorded the output of CSE in two cases to ensure that the output of the CSE did not depend on the diameter (and therefore impedance) of the output electrodes. In one case the CSE was connected to the bath with large caliber surgical tubing and in the other case we used the microcatheter electrodes shown in Figure 2C. The latter case is diagrammed in Figure 2B.

To test the SDCS1's ability to drive direct ionic current at the output of the system using AC at the metal electrodes, we measured ionic current flow using the CSE through a saline bath emulating stimulated tissue under 3 conditions: (1) all valves closed (which should block all current flow), (2) A valves open and B valves closed (which should yield a square wave AC ionic current, and (3) normal operation with valves switching in synchrony with the square wave driving current applied to the electrodes (which should yield DC ionic current).

B. SDCS1 and safe DC Neural Modulation in vivo

While SCDS is a general-purpose stimulation technology with potentially broad applications, our goal in the present study was to characterize the SDCS1's performance using an already well-characterized in vivo preparation that could benefit from the additional capabilities DC allows. We therefore studied the use of DC modulation in application to prosthetic stimulation of the vestibular nerve, an application with which we have significant experience [21–36] and for which SCDS1's ability to inhibit spontaneous activity would be especially advantageous.

Normally, the vestibular system helps the eyes maintain visual acuity by stabilizing gaze via the vestibulo-ocular reflex (VOR) during head rotations in any direction using sensory input from the vestibular labyrinths in both ears. Sensation of head rotation generates signals that control the extraocular muscles of each eye. In a normal chinchilla, vestibular nerve afferents maintain spontaneous firing at an average ~60 spikes/s [37]. Primary afferent neuron firing rates on one side of the head increase when the head rotates toward that side and decrease when the head rotates in the opposite direction. The VOR driven by these

changes in firing rate moves the eyes at same speed as the head but in the opposite direction. Three vestibular nerve branches in each inner ear deliver information from three orthogonally oriented semicircular canals (SCC) and encode head rotation about the three corresponding head rotation axes[12;38]. Monitoring eye movement velocity and direction is a sensitive, specific and efficient assay of vestibular nerve afferents' excitation and inhibition [39].

Five adult wild-type 450–650g chinchillas (Chinchilla lanigera) were studied. Surgical procedures were conducted in accordance with a protocol approved by the Johns Hopkins Animal Care and Use Committee and described in detail previously [26]. Only deviations from the previously published technique are detailed here. In brief, under general anesthesia a phenolic post for head restraint was positioned in the midline perpendicular to the skull at the bregma and embedded in dental cement extruded into each bulla.

One of the chinchillas was implanted with PtIr stimulating wire electrodes in each SCC of the left labyrinth. Twisted pairs of wire electrodes (Fig. 2C) were implanted for redundancy, but only one was wire used at any one time for stimulation. A monopolar near reference electrode was placed in the common crus and an alternate distant reference electrode was placed in neck musculature. In the other four chinchillas, saline/agar tube electrodes (Fig. 2C) were implanted in the vestibular labyrinths instead of PtIr wire electrodes. The small outer diameter of the tubes (~150μm) allows intralabyrinthine implantation near the SCC branches of the vestibular nerve [40]. A total of 5 tube electrodes were implanted: one in each of the three SCCs, one near reference in the vestibule, and one distant reference in neck musculature. Electrodes were secured using dental cement. Plugs in each tube and a plastic cap attached to the phenolic post protected the tube electrodes between experiments.

A real-time, binocular 3-dimensional video-oculography (3D VOG) system modified slightly from one described previously in detail [34] was used for recording eye movements in response to electrical stimulation of the SCCs. In brief, an array of three fluorescent yellow squares on a black film was placed on the topically anesthetized cornea of each eye using a small amount of veterinary tissue glue (VetBond, 3M) after application of proparacaine, pilocarpine and saline eye drops. Firewire cameras (Dragonfly Express, Point Grey Research) retrofitted with 25 mm focal length, f/2.0 microvideo lenses were used to acquire 500×400 pixel images at 179 Hz for each eye using custom software. The output of this system indicates the eye velocity about each of three axes corresponding approximately to the axes of the semicircular canals: horizontal (H), left anterior/right posterior (LARP), and right anterior/left posterior (RALP).

1) DC Stimulation Safety—To test the ability of the tube electrodes alone (independent of the SCDS1) to safely conduct DC ionic current in vivo for a prolonged duration, we used an AM2200 to deliver DC via large surface area metal electrodes inserted into shanks of tube electrodes in one animal. In this case, rather than having the tube electrodes submerged in a saline bath as in Fig. 2B, one was implanted in the left anterior SCC near the vestibular nerve, and a return tube electrode was positioned in the vestibule farther away from the vestibular nerve. We hypothesized that long duration DC stimuli via the tubes would not cause a subsequent degradation in performance due to electrode polarization or neural

damage, because of the large electrode surface area and long distance between the metal/saline interface and neural tissue in this preparation. We recorded VOR eye responses to steps in DC current (1s duration, 0–80μA, anodic at the active electrode) before and after delivering 15000s of 80μA anodic DC, interrupted occasionally to ensure the animal was not adversely affected by the stimulus. We chose 80μA amplitude because this step in DC from 0μA evokes strong VOR eye movements without evoking twitches of facial musculature that indicate spurious facial nerve stimulation. We conducted paired t-tests to compare the magnitude and axis of VOR eye rotation in response to the test stimuli before and after the long duration DC presentation.

To confirm that observation of eye movement can detect acute injury due to passage of "unsafe" DC, we recorded eye movements during and after delivery of 10s steps of 40μA anodic and then 10s steps of 40μA cathodic DC to one chinchilla via standard PtIr wire electrodes of ~235μm^2 metal/saline interface area. To limit potential discomfort to the animal we conducted 5 iterations of each stimulus presentation because the 40μA current needed to evoke VOR activity required current density of 14000$\mu C/cm^2$, which is over 100× greater than the ~100$\mu C/cm^2$ standard electrochemical safety constraints for the PtIr electrodes [3].

2) DC Suppression of Spontaneous Vestibular Nerve Activity—Vestibular prostheses encode head rotation by sensing head velocity with head-fixed gyroscopes and modulating activity on corresponding branches of the vestibular nerve. The standard pulse frequency modulation (PFM) stimulation paradigm used in these devices can readily increase firing rates to encode head rotation toward the implanted side of the head, but encoding head movement away from the implanted side is more challenging, because spontaneous activity sets a floor beneath which an excitatory stimulator cannot down-modulate the nerve. We hypothesized that delivering anodic DC to inhibit spontaneous activity concurrently with PFM would improve the VOR response compared to PFM stimulation alone.

Three chinchillas received pulsatile stimulation delivered via a tube electrode in the left posterior SCC near the posterior ampullary branch of the vestibular nerve. We delivered 60 pulses per second (pps) baseline pulsatile stimulation to the tube electrode using a multichannel vestibular prosthesis with the reference electrode positioned in neck muscles. We then applied 500ms steps in pulse rate from the 60pps baseline in 2s intervals alternating between upward steps (of 100, 200 and 300pps) and downward steps (of 20, 40 and 60pps). VOR responses to 5 steps of each size were acquired. This rate modulation paradigm was then repeated while anodic DC was constantly applied through large-area metal electrodes via the same tube electrodes used to deliver PFM stimulation.

Current amplitude for the 200μs/phase pulsatile stimuli was set at the start of the experiment for each chinchilla by observing VOR responses during 0pps-to-400pps step modulation. The amplitude was set at ~66% of the way between the threshold eliciting VOR responses and threshold eliciting facial muscle contraction. These amplitudes were 120, 200 and 250μA/phase for chinchillas ch408, ch406, and ch407, respectively. A similar procedure was conducted for the DC stimulation amplitude, resulting in DC stimulation amplitudes set to

100, 80 and 50μA, respectively. Once current amplitudes were set for each chinchilla, they were kept constant throughout the experiment.

3) SDCS1 Modulation of the Vestibular Nerve—Goldberg et al showed that anodic DC applied via a relatively large silver electrode positioned in perilymph in the inner ear inhibits vestibular primary afferent neuron activity, and that cathodic stimulation excites it [41]. In those studies, the duration of DC current application was limited to 5s due to charge-injection constraints and electrode polarization. To determine whether the SDCS1 can inhibit and excite neural activity in an analogous in vivo preparation but using implanted tube electrodes, we delivered 5s pulses of anodic or cathodic currents using SDCS1 connected to a tube electrode positioned near the horizontal branch of the vestibular nerve with the reference tube electrode positioned in neck musculature. We recorded eye movements and monitored the output of the device using the CSE. We expected VOR eye movements to be consistent with vestibular nerve inhibition during anodic stimulation and excitation during cathodic stimulation.

IV. Results

A. Bench Test

The CSE voltage response to ionic current driven through it is shown in Fig. 3A. As expected, the voltage across the CSE shows a linear relationship to the DC current through it. The CSE voltage when the current was delivered using tube electrodes rather than large-caliber surgical tubing is indicated with red dots on the calibration curve. The CSE accurately tracks electrical current flowing through it for both large caliber, low impedance surgical tubing and for the high impedance tube electrodes used for animal experimentation.

When all valves are closed, current is prevented from flowing to the tissue (Fig. 3B). When one set of the valves is held open, the device freely conducts current in both directions (Fig. 3C). When the SDCS1 is allowed to operate properly, it delivers rectified ionic DC; however; current flow is interrupted periodically at each phase transition of the AC waveform controlling the device (Fig. 3C). These interruptions are 10–50ms long and most likely result from non-ideal valve behavior. Valve transitions are not instantaneous, so complementary valves can be briefly but simultaneously both open or both shut, causing open or short circuits through the ionic bridge. Both conditions interrupt current flow through the stimulated tissue.

B. Neural Modulation

1) DC Stimulation Safety—Delivering 40μA DC stimulation via 235μm^2 Pt/Ir (metal) microelectrodes for long duration was not possible without degrading VOR responses. After 4 presentations of either anodic or cathodic “unsafe DC” over 10s, the animal would exhibit a brisk post-stimulation nystagmus (indicative of disruption of normal activity in the implanted labyrinth) lasting 5–15min, probably due to hydrolysis at the active electrode, which generates bubbles of hydrogen at cathodes and oxygen at anodes.

In contrast, responses to steps in DC current made safe by delivery via tube electrodes did not change even after over 15000s of continual 80μA presentation of anodic DC (Fig. 4).

There was an initial nystagmus associated with the step in long duration DC stimulation that diminished with adaptation within ~60s of stimulation. We did not observe any aberrant VOR responses to test stimuli during the safe DC (SDC) experiment or after 15000s of continual DC. Sample responses to stimulation at the beginning and end of the experiment are shown. Neither response amplitude nor response axis changed significantly from before to after the 15000s of continual DC (paired t: $P>0.87$ for amplitude; $P>0.63$ for angle between initial and final axis of eye rotation).

2) DC Suppression of Spontaneous Nerve Activity—Concurrent DC + PFM increased the dynamic range of both inhibitory and excitatory VOR response compared to PFM without DC stimulation (Fig. 5). For each of the three chinchillas, ch408, ch406, and ch407, maximum inhibitory VOR responses to a 60pps downward step from baseline pulse rate without DC stimulation were 32±5°/s, 15±5°/s, and 15±7°/s. Responses to the same step improved during concurrent DC to 63±8°/s, 19±4°/s, and 22±12°/s, respectively. Maximum excitatory VOR eye movements in response to a 300pps increase from baseline without DC stimulation were 174±25°/s, 212±6°/s, and 92±13°/s. Responses to the same increase in pulse rate improved with DC stimulation to 289±18°/s, 352±14°/s, and 147±6°/s. Results for chinchilla ch408 are presented in Figure 5A for both decrease (plot on the left) and increase (plot on the right) in pulse rate from the 60pps baseline. When data were aggregated for all three chinchillas (Fig. 5B), a significant increase in VOR dynamic range with concurrent DC stimulation is apparent both when the pulse rate was decreased by the maximum possible step of 60pps (ANOVA $F=25$, post-hoc t-test $P<0.03$) and when the pulse rate was increased by the maximum possible step of 300pps (ANOVA $F=334$, post-hoc t-test $P<10-6$).

3) SDCS1 Modulation of the Vestibular Nerve—To test the ability of the SDCS1 to both suppress and excite the vestibular nerve we delivered anodic and cathodic pulses to the tube electrode implanted near the horizontal branch of the vestibular nerve. Fig. 6 shows VOR responses confirming that cathodic SDC excites and anodic SDC inhibits vestibular nerve activity. Insets in Fig. 6 show sample horizontal VOR eye velocity traces of chinchilla ch406 in response to a 35μA cathodic step (upper left of the inset) and a 70μA anodic step (lower right of the inset). The cathodic response in the inset reaches a peak slow-phase leftward velocity of 270°/s. The occasional rapid velocity spikes in the opposite direction indicate nystagmus quick phases, which are non-VOR eye movements that reset eye position when the eye reaches the limit of its movement range.

V. Discussion

We presented the concept, initial safety and efficacy data, and a working prototype for a safe DC neural modulation system. The SDCS1 system delivers ionic DC via flexible microcatheter tube electrodes. It accomplishes this by switching mechanical valves in phase with AC square wave currents applied to metal electrodes immersed in the ionic solution of a bridge rectifier. Whereas passage of unsafe DC into the vestibular labyrinth via traditional metal microelectrodes elicited signs of inner ear injury within ~40 seconds of onset, safe DC presented via saline-bridge tube microelectrodes elicited no signs of injury even after presentations lasting 15000s, or >3 orders of magnitude above the duration allowed by classic safe charge injection constraints.

We demonstrated the efficacy of SDC as an adjunct to traditional vestibular prosthesis stimulation paradigms, which have so far been based on PFM alone. Concurrent DC+PFM stimulation, in which SDC is used to reduce or silence natural spontaneous activity so that traditional PFM stimuli can more completely control vestibular afferent firing rates, improved both the inhibitory and excitatory dynamic range of VOR responses. Improvements we observed in VOR during DC+PFM are consistent with DC suppression of the vestibular nerve spontaneous activity. For inhibitory PFM stimuli, DC suppression likely facilitated PFM encoding by driving afferent spontaneous activity down, allowing down-modulation of PFM rates to better mimic normal encoding of inhibitory head movements. For excitatory PFM stimuli, DC suppression likely facilitated PFM encoding allowing up-modulation of PFM rates to start from a lower effective baseline (i.e., the 60pps PFM baseline, rather than the combination of baseline PFM and spontaneous activity), avoiding the lower sensitivity region of the sigmoidal VOR/spike rate relationship, which saturates at higher spike rates [37].

We also demonstrated that safe DC alone, delivered by the prototype SDCS1 system, can also evoke both excitatory and inhibitory VOR responses. As expected, the dynamic range for inhibitory SDC is ~1/3 of the range for excitatory SDC. This is probably because vestibular afferents normally maintain a spontaneous rate of ~60sp/s; excitation with cathodic DC can increase this rate up to ~350sp/s, but inhibition with anodic DC can only decrease it to 0sp/s.

A. Opportunities for Device Improvement

SDCS1 in its present form presents several technical challenges to overcome before the SDCS concept can be extended to chronic neuromodulation experiments. First, it is constrained to steps of DC and does not programmatically change polarity or amplitude of the ionic current. Because it is built using laboratory bench equipment and is therefore physically large, it is not easily applied to chronic experiments. Additionally, the fidelity of the DC system output is degraded by periodic interruptions in current flow due to non-ideal behavior of SCDS1's mechanical valves. These 10–50ms interruptions can evoke volleys of neural activity with each valve transition.

Interruptions in current flow occur because ionic current does not reach tissue when complementary valves are both open or both closed during valve transitions. For example, if A1 and B1 in Fig. 1 are both closed during a transition, no current will flow through the tissue. Faster valves could shorten the duration of current interruptions but would not completely eliminate them. A second-generation SDCS now being developed, the SDCS2, could resolve this problem by effectively running two SDCS1 systems in tandem. In this scheme, while SDCS1A drives current through the tissue, SDCS1B's current source turns off and SDCS1B's valves then switch state. Once the SDCS1B valve transition is complete, SDCS1B energizes its current source, assuming control so that SDCS1A can deactivate its current source prior to switching its valves. This method should prevent interruptions in current flow even with relatively slow valves.

Apart from improving the stability of purely DC stimuli, overcoming the problem of transient interruptions in ionic flow would also allow an SDCS system to deliver time-

varying, non-DC, cathodic and anodic analog stimulus waveforms by running the system with a relatively high-frequency, pulse-amplitude-modulated square wave current source. Although this would offer no major benefit over traditional metal microelectrodes when the analog stimulus waveforms of interest are of high enough frequency to allow adherence to safe charge injection criteria (e.g., as used in early cochlear implants employing the "sinusoidal analog stimulation" [SAS] paradigm with audio frequency stimuli) [42], a "low frequency AC" variant of SDC would allow the use of analog stimulus waveforms in vestibular prostheses, retinal prostheses and other settings in which the analog signals of interest are well below ~1kHz.

The entire system should be miniaturized for wearability (e.g., through incorporation of microfluidic MEMS technology [43]) and battery operation during chronic animal testing. CSE output should provide feedback to a control circuit that adjusts voltage-controlled current sources to ensure constant current at the output of the device. The device should be self-contained and modularized, so that it can serve as a general purpose "back-end" to deliver safe direct current stimulation for a variety of neural control applications.

Differences in the ionic flow paths available in different tissues mandate that SDCS safety be assessed individually for each therapeutic application. SDCS1 can be thought of as an ion pump that pulls in cations through one tube electrode and deposits them from the other, while shuttling anions in the opposite direction. Since this device does not differentiate between different species of cations or anions, the precise anatomic locations of tube electrodes are important. For example, if one tube electrode is positioned in a high Na+, low K+ concentration environment (like the inner ear's perilymphatic spaces) and the other electrode is positioned in a separate compartment with high K+, low Na+ concentration (like endolymph), then the SDCS could alter the ionic make-up of the two fluids over time. This problem should be avoided by implanting the two tube electrodes as a bipolar pair in a homogeneous environment that does not interpose an impermeable membrane between the two tubes. Several potential sites of application that satisfy this criterion are discussed below.

B. Potential Applications

Passage of DC from a chronically implanted medical device has long been considered off limits and undesirable. Indeed, it is usually a harbinger of impending device failure and/or tissue injury. The advent of safe DC could fundamentally change how biomedical engineers design neural prostheses and how clinicians and implant recipients use them. Most importantly, using safe DC to modulate neural activity could expand the capabilities of chronically implanted neural prostheses to previously unapproachable applications.

1) Vestibular Prosthesis—As described earlier, the standard PFM stimulation paradigm used in vestibular prostheses can readily increase firing rates to encode head rotation toward the implanted side of the head, but encoding head movement away from the implanted side is more challenging, because spontaneous activity sets a floor beneath which an excitatory stimulator cannot down-modulate the nerve. The most common solution to this problem has been to adapt the vestibular system to an artificially high baseline pulse rate from which

subsequent withdrawals of excitation can encode inhibition. Unfortunately, the resulting increase in inhibitory dynamic range can be accompanied by a decrease in excitatory dynamic range [25;44].

We did not use SDCS1 for DC+PFM stimulation experiments due to periodic interruptions in ionic flow inherent to the SDCS1's components. However, our extended duration stimulation experiment confirms that DC can be delivered for very long periods through tube electrodes without eliciting signs of inner ear injury, and our DC+PFM results show that DC can enhance the function of a traditional biphasic pulsatile stimulator, most likely by reducing or silencing normal spontaneous activity.

2) Pain Control—Conventional treatments for chronic neuropathic pain consist primarily of opiate analgesics and implanted stimulators employing charge-balanced AC pulses. Systemic drug treatments have adverse effects such as depression, sedation, dizziness, nausea, itching, and constipation along with risks of addiction, abuse and reduced efficacy over time [45]. Spinal cord stimulators do not have these side effects, but only ~50% of patients using them report adequate pain control, and many report paresthesia (abnormal sensation due to interference with proprioceptive and somatosensory signals) [46]. Spinal cord stimulators are thought to inhibit pain indirectly through a gate-control mechanism by exciting large dorsal column fibers. These fibers have inhibitory and modulatory projections that interfere with pain propagation through the dorsal laminae of the spinal cord.

Pain is conducted by C and Aδ fibers, which are the smallest diameter fibers in peripheral nerves. Because small diameter fibers have higher electrical thresholds than larger diameter fibers, they cannot be selectively shut down by anodic DC stimulation from an SDCS without changes in activity of larger fibers. However, the course of C and Aδ fibers separates from the rest of a peripheral nerve near the spinal cord dorsal root entry zone (DREZ). Surgical destruction of fibers at the DREZ was shown to relieve intractable pain in 76% of patients affected with peripheral nerve avulsions [47]. However this approach is invasive, irreversible and associated with a risk of serious complications.

Anodic safe DC delivered via tube electrodes near the DREZ (with return tubes in cerebrospinal fluid elsewhere in the spinal canal) could chronically inhibit pain transmission. This reversible approach could offer significant advantages: it could result in more effective suppression of pain with fewer side effects than drug treatments, less paresthesia than traditional AC spinal cord stimulators, and less loss of normal function than surgical destruction.

3) Cortical Stimulation—Transcranial direct current stimulation (tDCS) has demonstrated beneficial effects in a wide range of pathologic conditions, such as stroke, epilepsy, chronic depression, drug cravings, and chronic pain from conditions such as fibromyalgia [48]. However, tDCS cannot be delivered continually, and effects of tDCS are relatively short lived, commonly lasting only for a few tens of minutes. Experimental evidence suggests that the primary mechanism of tDCS is modulation of resting membrane potential in cortical interneurons, making these cells more or less excitable to natural stimuli [48]. SDCS offers a possible alternative to tDCS in that SDCS can chronically deliver

excitatory or inhibitory direct current modulation. Whereas tDCS has limited spatial resolution, a chronically implanted, self-contained SDCS could offer neuromodulatory control in spatially localized areas of the cortex accessed via small diameter tube electrodes.

4) Auditory Prosthesis—Low amplitude cathodic SDC extracellular current chronically delivered to the afferent fibers of the auditory nerve could partially depolarize their membranes, making them more likely to generate an action potential in response to excitation from the inner hair cells and thus making them more sensitive to incoming sound. No signal modulation would be required for this prosthesis, because the cathodic SDC current only needs to enhance the sensitivity of the afferent fibers to neurotransmitter release evoked naturally by sound (but to a lesser degree in a diseased ear than normal). This concept for an auditory “sensitizer” could provide a powerful adjunct or alternative to other electroacoustic hearing devices [49] used to treat hearing loss and tinnitus.

Spelman and colleagues attempted to apply their original SDC design to the cochlea in rodents, placing anodic and cathodic pipette electrodes in the endolymphatic and perilymphatic compartments, respectively, with the goal of enhancing the endocochlear potential between these compartments (which is deficient in certain types of cochlear hearing loss) [17;18;50]. They found that the approach did in fact elevate the endocochlear potential as expected, but signs of failing cochlear health became apparent within ~10 min. In retrospect, damage may have occurred because the ion pumping effect of SDC disrupted the normal ionic concentrations in the different compartments. A redesigned bipolar tube electrode array that keeps all tube orifices in the same compartment (e.g., scala tympani) might avoid the problems encountered by Spelman, et al. Wide separation between anodic and cathodic openings and differences in tube orifice diameter could be used to sculpt the current density profile along the cochlea.

5) Paralysis and the Inverse Recruitment Problem—One of the oldest problems in neural engineering has been the “inverse recruitment problem” [51]. Normally, when a motor nerve commands muscles to contract, the muscles are activated in sequence from the smallest to the largest fibers. The smallest nerve fibers innervate the smallest muscle fibers and largest motor neurons innervate the largest muscle fibers. Unfortunately, small caliber neurons have higher electrical activation thresholds than large caliber neurons, so when a traditional neuroelectronic prosthesis attempts to contract a muscle group by applying pulsatile stimulation to the corresponding motor nerve, the muscle’s recruitment order is opposite of the natural order. This inverse recruitment order results in coarse, unnatural movements and muscle fatigue [52].

SDCS can be used to restore a more natural recruitment order. Like biphasic pulses, DC also affects neurons in “reverse” order [53]; however, DC’s ability to inhibit allows one to turn this effect into an advantage. In one approach, a standard pulsatile electrode pair could be positioned proximally on a motor nerve while an anodic SDCS electrode is positioned more distally. The proximal pulsatile stimulating electrode is set up to chronically deliver high rate, high amplitude stimulation engendering high firing rates on most or all fibers in the nerve. The distal SDCS can then apply anodic current to inhibit the motoneurons more distally. High amplitude SDCS current should suppress action potential propagation in all

but the smallest diameter motor neurons. As the SDCS anodic current is reduced under control of a signal intended to command contractile force, smaller fibers are the first to be freed from the anodic block, followed by larger and larger motor fibers. Thus, a more normal recruitment pattern is restored at the muscle.

VI. Conclusions

We designed and built a prototype safe direct current neural stimulator system that delivers direct ionic current via microcatheter tubes filled with ionic gel. Bench tests indicate that the system indeed delivers DC at the output of the system when AC pulses are delivered to each of two metal electrodes within the stimulator. Experimental data obtained in chinchillas suggest that long duration (>15000s) direct current applied to the vestibular nerve via microcatheter tube electrodes did not cause damage to the target neurons, whereas deliver of the same current via similarly sized traditional Pt/Ir metal microelectrodes implanted directly in the ear elicit signs of biologic injury within ~40s. Whereas traditional biphasic pulse based stimulators can generally only excite nearby nerves, vestibulo-ocular reflex eye movements in response to cathodic and anodic DC delivered by the SDCS confirm the system's ability to both excite and inhibit neuronal activity. While multiple aspects of the device design and construction will require modification prior to chronic application, the SDC approach could open a new realm of possibilities for the design and application of neuroelectronic prostheses.

Acknowledgments

This work was supported in part by the NIH grant R01-DC009255. We would like to thank Francis Spelman and Scott Corbett for sharing their experience and insight, the members of the Johns Hopkins Vestibular NeuroEngineering Laboratory for helpful discussions and support throughout the effort, Yun Guan and Srinivasa Raja for the discussions regarding using SDCS technology for the treatment of chronic pain, and Andrew Chang and Irving Reti for discussion regarding potential cortical applications. The authors are inventors on patents related to technology discussed in this article, and CCDS is an owner and CEO of Labyrinth Devices LLC, a company founded to support commercialization of vestibular prosthesis technology.

References

1. Guenther T, Lovell NH, Suaning GJ. Bionic vision: system architectures: a review. Expert. Rev. Med. Devices. 2012 Jan.9(no. 1):33–48. [PubMed: 22145839]
2. Wilson BS, Dorman MF. Cochlear implants: a remarkable past and a brilliant future. Hear. Res. 2008 Aug.242(no. 1–2):3–21. [PubMed: 18616994]
3. Merrill DR, Bikson M, Jefferys JGR. Electrical stimulation of excitable tissue: design of efficacious and safe protocols. Journal of Neuroscience Methods. 2005; 141(no. 2)
4. Robblee, L.; Rose, T. Electrochemical guidelines for selection of protocols and electrode materials for neural stimulation. In: McCreary, DB.; Agnew, WF., editors. Neural Prostheses: Fundamental Studies. Prentice-Hall; 2003.
5. Rose TL, Robblee LS. Electrical-Stimulation with Pt Electrodes .8. Electrochemically Safe Charge Injection Limits with 0.2 Ms Pulses. IEEE Transactions on Biomedical Engineering. 1990; 37(no. 11)
6. Deniau JM, Degos B, Bosch C, Maurice N. Deep brain stimulation mechanisms: beyond the concept of local functional inhibition. Eur. J. Neurosci. 2010 Oct.32(no. 7):1080–1091. [PubMed: 21039947]
7. Meyerson BA, Linderoth B. Mode of action of spinal cord stimulation in neuropathic pain. J. Pain Symptom. Manage. 2006 Apr.31 Suppl(no. 4):S6–S12. [PubMed: 16647596]

8. Melzack R, Wall PD. Pain mechanisms: a new theory. Science. 1965 Nov.150(no. 3699):971–979. [PubMed: 5320816]
9. Ackermann DM Jr, Bhadra N, Foldes EL, Kilgore KL. Conduction block of whole nerve without onset firing using combined high frequency and direct current. Med. Biol. Eng Comput. 2011 Feb. 49(no. 2):241–251. [PubMed: 20890673]
10. Bhadra N, Bhadra N, Kilgore K, Gustafson KJ. High frequency electrical conduction block of the pudendal nerve. J. Neural Eng. 2006 Jun; 3(no. 2):180–187. [PubMed: 16705274]
11. Boger A, Bhadra N, Gustafson KJ. Bladder voiding by combined high frequency electrical pudendal nerve block and sacral root stimulation. Neurourol. Urodyn. 2008; 27(no. 5):435–439. [PubMed: 18041769]
12. Carey, JP.; Della Santina, CC. Principles of applied vestibular physiology. In: Cummings, CW., editor. Otolaryngology - Head & Neck Surgery. Elsevier; 2005.
13. Aran JM, Cazals Y. Electrical suppression of tinnitus. Ciba Found. Symp. 1981; 85:217–231. [PubMed: 6976888]
14. Luedtke K, Rushton A, Wright C, Juergens TP, Mueller G, May A. Effectiveness of anodal transcranial direct current stimulation in patients with chronic low back pain: Design, method and protocol for a randomised controlled trial. BMC. Musculoskelet. Disord. 2011 Dec.12(no. 1):290. [PubMed: 22204615]
15. Jiruska P, Bragin A. High-frequency activity in experimental and clinical epileptic foci. Epilepsy Res. 2011 Dec.97(no. 3):300–307. [PubMed: 22024189]
16. Senning A. Developments in cardiac surgery in Stockholm during the mid and late 1950s. J. Thorac. Cardiovasc. Surg. 1989 Nov.98(no. 5 Pt 2):825–832. [PubMed: 2682018]
17. Spelman F. Electrodes and Stimulators for Strial Presbycusis. Thirty Fourth Neural Prosthesis Workshop. 2003
18. Spelman, FA.; Johnson, TJ.; Corbett, SS.; Clopton, BM. Apparatus and Method for Treating Strial Hearing Loss. US Pat. 6,694,190 B1. 2004 Feb..
19. Ackermann DM Jr, Bhadra N, Foldes EL, Kilgore KL. Separated interface nerve electrode prevents direct current induced nerve damage. J. Neurosci. Methods. 2011 Sept.201(no. 1):173–176. [PubMed: 21276819]
20. Sewell WF, Borenstein JT, Chen Z, Fiering J, Handzel O, Holmboe M, Kim ES, Kujawa SG, McKenna MJ, Mescher MM, Murphy B, Swan EE, Peppi M, Tao S. Development of a microfluidics-based intracochlear drug delivery device. Audiol. Neurootol. 2009; 14(no. 6):411–422. [PubMed: 19923811]
21. Chiang B, Fridman GY, Dai C, Rahman MA, Della Santina C. Design and performance of a multichannel vestibular prosthesis that restores semicircular canal sensation in macaques. IEEE Trans. Neural Syst. Rehabil. Eng. 2011 Oct; 19(5):588–598. [PubMed: 21859631]
22. Dai C, Fridman GY, Chiang B, Davidovics NS, Melvin TA, Cullen KE, Della Santina CC. Cross-axis adaptation improves 3D vestibulo-ocular reflex alignment during chronic stimulation via a head-mounted multichannel vestibular prosthesis. Exp. Brain Res. 2011 May; 210(no. 3–4):595–606. [PubMed: 21374081]
23. Dai C, Fridman GY, Della Santina CC. Effects of vestibular prosthesis electrode implantation and stimulation on hearing in rhesus monkeys. Hear. Res. 2010 Dec.
24. Dai C, Fridman GY, Davidovics NS, Chiang B, Ahn JH, Della Santina CC. Restoration of 3D vestibular sensation in rhesus monkeys using a multichannel vestibular prosthesis. Hear. Res. 2011 Aug.
25. Davidovics N, Fridman GY, Della Santina CC. Effects of Baseline Stimulation While Modulating Pulse Rate and Current Amplitude in Vestibular Prosthesis. Assoc. Research in Otolaryngology Midwinter Meeting. 2011
26. Della Santina CC, Migliaccio AA, Patel AH. A multichannel semicircular canal neural prosthesis using electrical stimulation to restore 3-D vestibular sensation. IEEE Transactions on Biomedical Engineering. 2007; 54(no. 6)
27. Della Santina CC, Migliaccio AA, Hayden R, Melvin TA, Fridman GY, Chiang B, Davidovics NS, Dai C, Carey JP, Minor LB, Anderson ICW, Park H, Lyford-Pike S, Tang S. Current and future

management of bilateral loss of vestibular sensation - an update on the Johns Hopkins multichannel vestibular prosthesis project. 2010

28. Della Santina CC. Regaining balance with bionic ears. Sci. Am. 2010 Apr.302(no. 4):68–71. [PubMed: 20349578]
29. Della Santina CC, Migliaccio AA, Minor LB. Vestibulo - ocular reflex of chinchilla during high frequency head rotation and electrical stimuli. Society for Neuroscience Abstract Viewer and Itinerary Planner. 2003; 2003
30. Fridman GY, Davidovics NS, Dai C, Migliaccio AA, Della Santina CC. Vestibulo-ocular reflex responses to a multichannel vestibular prosthesis incorporating a 3D coordinate transformation for correction of misalignment. J. Assoc. Res. Otolaryngol. 2010 Sept.11(no. 3):367–381. [PubMed: 20177732]
31. Hayden R, Sawyer S, Frey E, Mori S, Migliaccio AA, Della Santina CC. Virtual labyrinth model of vestibular afferent excitation via implanted electrodes: validation and application to design of a multichannel vestibular prosthesis. Exp. Brain Res. 2011 May; 210(no. 3–4):623–640. [PubMed: 21380738]
32. Hullar TE, Della Santina CC, Hirvonen TP, Lasker DM, Carey JP, Minor LB. Responses of Irregularly Discharging Chinchilla Semicircular Canal Vestibular-Nerve Afferents During High-Frequency Head Rotations. J Neurophysiol. 2004 Dec.
33. Melvin TA, Della Santina CC, Carey JP, Migliaccio AA. The effects of cochlear implantation on vestibular function. Otol. Neurotol. 2009 Jan.30(no. 1):87–94. [PubMed: 19108038]
34. Migliaccio AA, MacDougall HG, Minor LB, Della Santina CC. Inexpensive system for real-time 3-dimensional video-oculography using a fluorescent marker array. Journal of Neuroscience Methods. 2005; 143(no. 2)
35. Sun, DQ.; Rahman, MA.; Fridman, GY.; Chiang, B.; Dai, C.; Della Santina, CC. Chronic Stimulation of the Semicircular Canals Using a Multichannel Prosthesis: Effects on Locomotion and Angular Vestibulo-Ocular Reflex in Chinchillas; Conf. Proc. IEEE 33rd Annual EMBC Conference; 2011.
36. Tang S, Melvin TAN, Della Santina CC. Effects of semicircular canal electrode implantation on hearing in chinchillas. Acta Oto-Laryngologica. 2009; 129(no. 5)
37. Baird RA, Desmadryl G, Fernandez C, Goldberg JM. The vestibular nerve of the chinchilla. II. Relation between afferent response properties and peripheral innervation patterns in the semicircular canals. Journal of Neurophysiology. 1988; 60(no. 1):182–203. [PubMed: 3404216]
38. Migliaccio AA, Minor LB, Della Santina CC. Adaptation of the vestibulo-ocular reflex for forward-eyed foveate vision. J. Physiol. 2010 Oct.588(no. Pt 20):3855–3867. [PubMed: 20724359]
39. Migliaccio AA, Minor LB, Della Santina CC. Adaptation of the vestibulo-ocular reflex for forward-eyed foveate vision. J. Physiol. 2010 Oct.588(no. Pt 20):3855–3867. [PubMed: 20724359]
40. Fridman GY, DellaSantina CC. Addition of Chronic Direct Current Stimulation Improves Vestibular Prosthesis Dynamic Range. Assoc. Research in Otolaryngology Midwinter Meeting. 2012
41. Goldberg JM, Smith CE, Fernandez C. Relation between discharge regularity and responses to externally applied galvanic currents in vestibular nerve afferents of the squirrel monkey. J. Neurophysiol. 1984 Jun; 51(no. 6):1236–1256. [PubMed: 6737029]
42. Xu L, Zwolan TA, Thompson CS, Pfingst BE. Efficacy of a cochlear implant simultaneous analog stimulation strategy coupled with a monopolar electrode configuration. Ann. Otol. Rhinol. Laryngol. 2005 Nov.114(no. 11):886–893. [PubMed: 16363059]
43. Oh KW, Ahn CH. A Review of Microvalves. J. Micromech. Microeng. 2006 Jan.2006(no. 16):R13–R39.
44. Merfeld DM, Haburcakova C, Gong W, Lewis RF. Chronic vestibulo-ocular reflexes evoked by a vestibular prosthesis. IEEE Transactions on Biomedical Engineering. 2007; 54(no. 6)
45. MacPherson RD. New directions in pain management. Drugs Today (Barc.). 2002 Feb.38(no. 2): 135–145. [PubMed: 12532190]

46. Carter ML. Spinal cord stimulation in chronic pain: a review of the evidence. Anaesth. Intensive Care. 2004 Feb.32(no. 1):11–21. [PubMed: 15058115]
47. Aichaoui F, Mertens P, Sindou M. Dorsal root entry zone lesioning for pain after brachial plexus avulsion: results with special emphasis on differential effects on the paroxysmal versus the continuous components. A prospective study in a 29-patient consecutive series. Pain. 2011 Aug. 152(no. 8):1923–1930. [PubMed: 21549506]
48. Stagg CJ, Nitsche MA. Physiological basis of transcranial direct current stimulation. Neuroscientist. 2011 Feb.17(no. 1):37–53. [PubMed: 21343407]
49. Gantz BJ, Turner CW. Combining acoustic and electrical hearing. Laryngoscope. 2003; 113(no. 10)
50. Spelman F, Corbertt S. personal communication to C. Della Santina. 2010 Oct.
51. Stieglitz T. Diameter-dependent excitation of peripheral nerve fibers by multipolar electrodes during electrical stimulation. Expert. Rev. Med. Devices. 2005 Mar.2(no. 2):149–152. [PubMed: 16293051]
52. Hamada T, Kimura T, Moritani T. Selective fatigue of fast motor units after electrically elicited muscle contractions. J. Electromyogr. Kinesiol. 2004 Oct.14(no. 5):531–538. [PubMed: 15301772]
53. Bhadra N, Kilgore KL. Direct current electrical conduction block of peripheral nerve. IEEE Trans. Neural Syst. Rehabil. Eng. 2004 Sept.12(no. 3):313–324. [PubMed: 15473193]

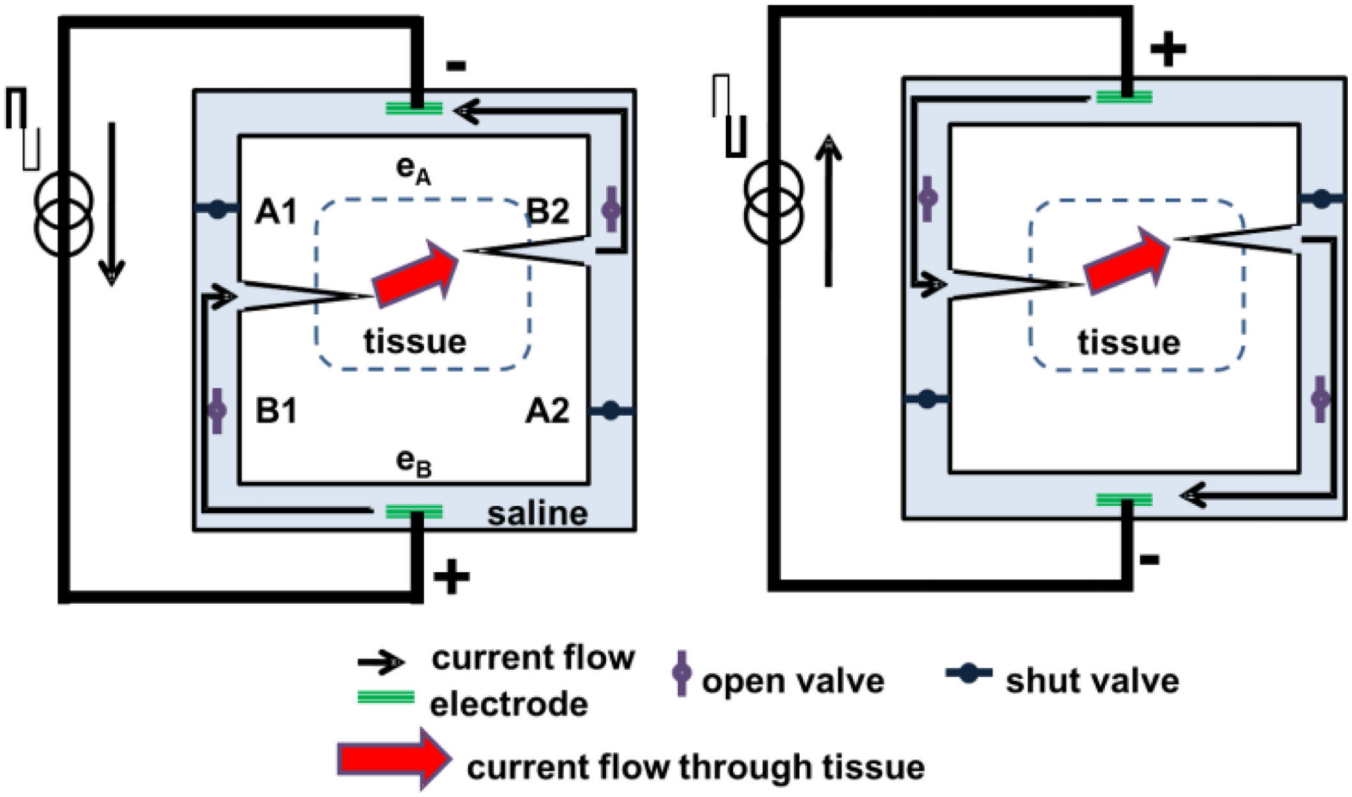

Figure 1.

SDCS concept. The two panels represent two states of the same device. (Left) Current flows from the lower electrode to the upper electrode. (Right) Current reverses direction, but because valves change state along with the electrical current direction, the ionic DC current (indicated by thick red arrow) still flows through the electrode tubes from left to right through the tissue. Valve A1 is always in the same state as valve A2 and valve B1 is always in the same state as valve B2, and all switch in synchrony with changes in electrode polarity.

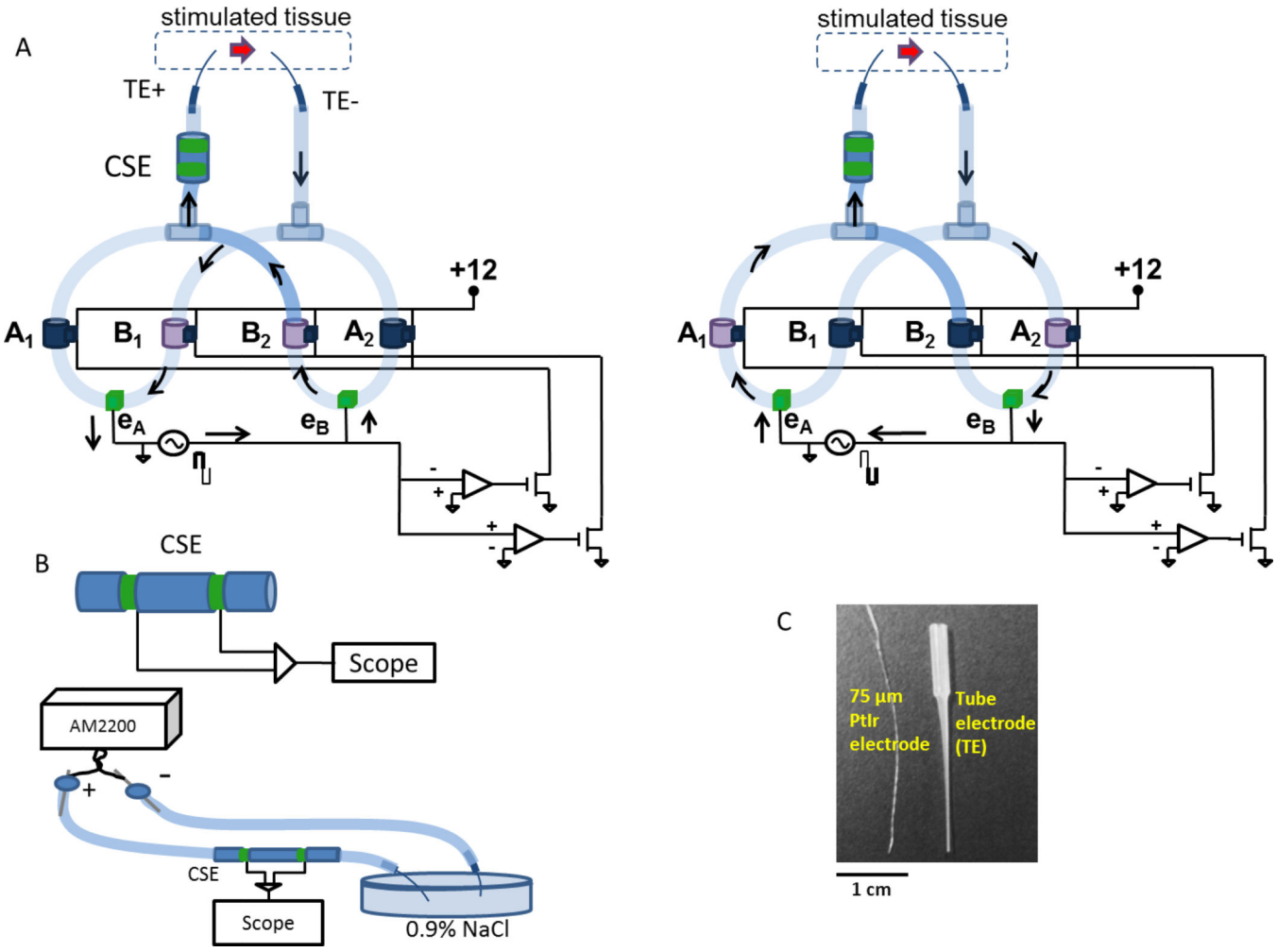

Figure 2.

SDCS1 prototype. (A) Two states of the system analogous to the schematic in Fig 1 are shown. Arrows indicate electric current flow. Open valves are light purple and shut valves are dark blue. The two tube electrodes (TE+ and TE−) deliver current to the tissue in the same direction in both system states indicated by the red arrow. Valves are interconnected with surgical tubing filled with 0.9% NaCl solution. Circuit at bottom right detects electrode voltage polarity and synchronously opens and closes valves in response to a square-wave AC signal is applied to electrodes e_A and e_B. (B) The output current is monitored using the CSE which differentially senses the voltage between two metal electrodes in contact with an ionic gel-filled salt bridge. The diagram shows calibration setup with tube electrodes, but calibration was also conducted with just surgical tubing inserted into the petri dish. AM2200 delivers controlled constant current via large surface area electrodes through the CSE and the voltage across the sensing electrodes is recorded with the scope. (C) Tube electrodes filled with ionic gel conduct ionic current from the SDCS but resist biological contamination and fluid flow, shown here in comparison with a twisted pair of 75µm PtIr wire electrodes commonly used for neural stimulation animal experiments.

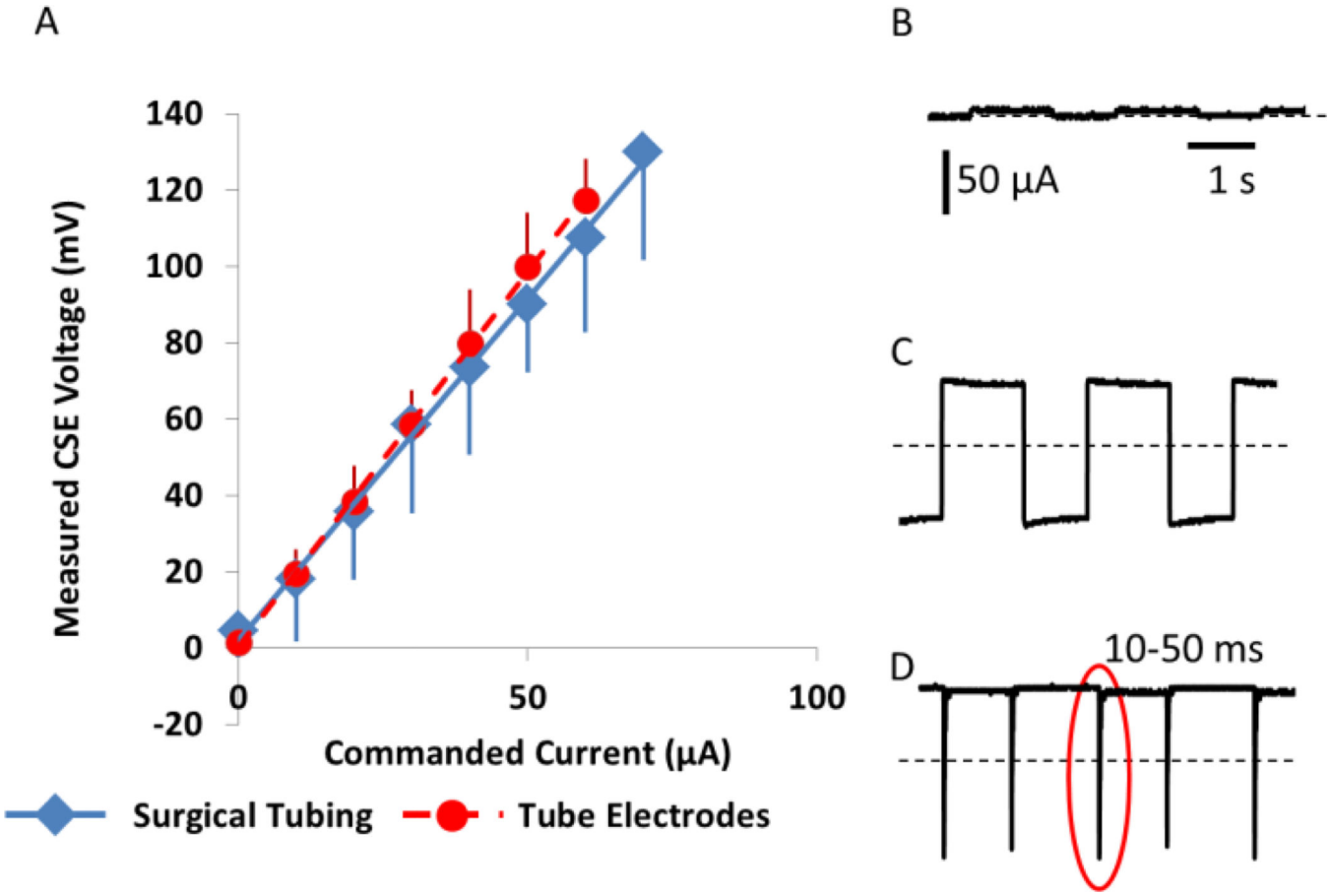

Figure 3.

SDCS1 bench tests. (A) CSE Calibration curve. (N=4) voltage-current relationship of the CSE did not change when tube electrodes were used at the output of the device instead of low impedance large diameter surgical tubing. (B) SDCS1 system output as measured by CSE is near 0 when all valves are closed. Current amplitude bar and time bar applies to B, C and D (C) Current flows in both directions when A valves are open and B valves are shut. (D) Approximately DC current when the valve driver circuit operates normally. Interruptions of output current flow due to non-ideal nature of the mechanical valve operation are apparent (one is within the oval). Interruptions are 10–50 ms long.

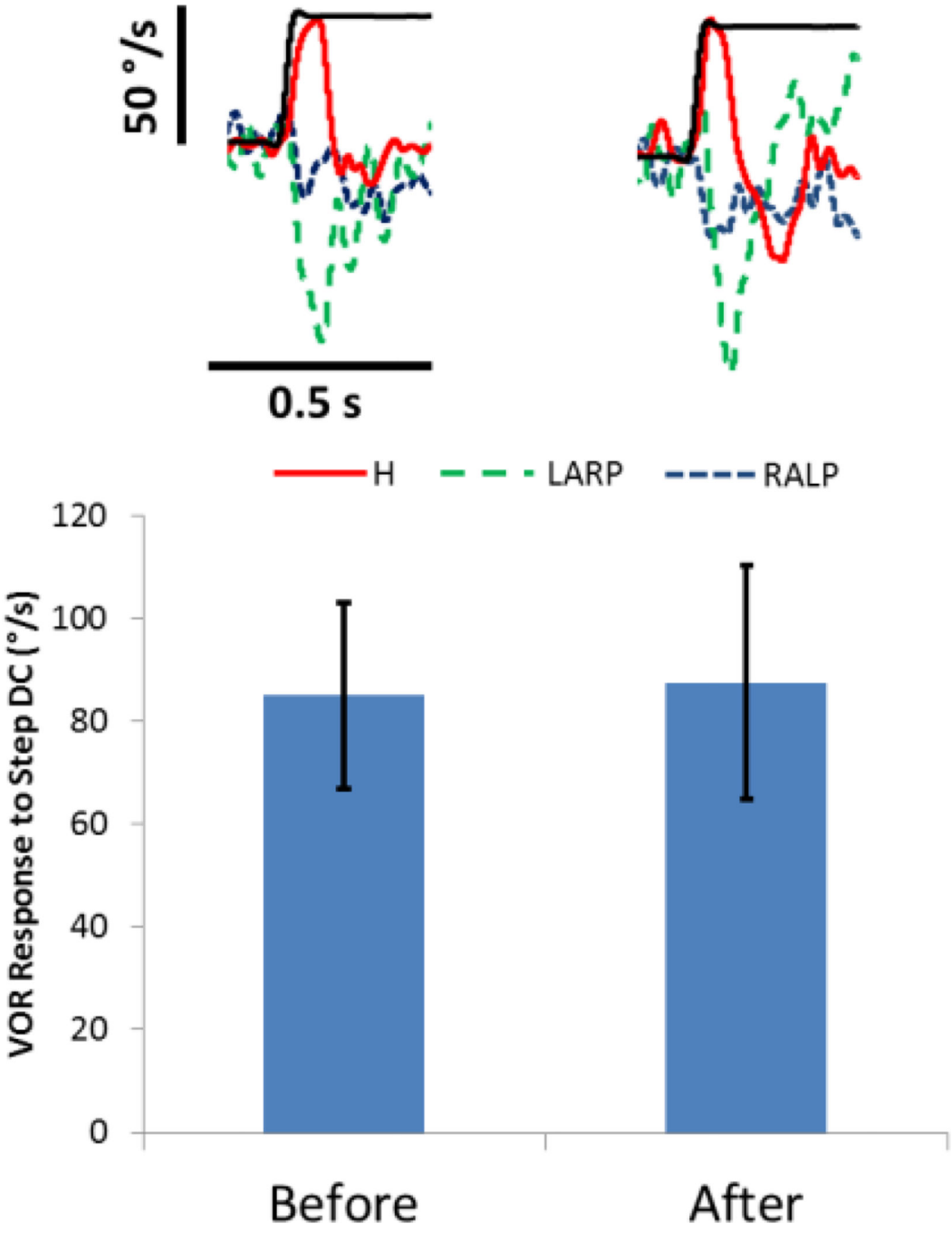

Figure 4.

Long term stimulation with 80uA safe DC current delivered via tube electrodes. An active tube electrode was implanted in the horizontal semicircular canal and a return tube electrode was implanted in the vestibule. Individual VOR responses show the three spatial components (red solid=Horizontal, green dashed =right anterior/left posterior, blue dotted = right anterior/left posterior) of the 3D VOR response to onset of a 80μA step in anodic DC (thin black) before (left) and after (right) the 15000s of 80μA anodic DC. The bar graph indicates the VOR responses to the 1s anodic DC test stimuli obtained before and after the

15000s of continual DC stimulation. VOR response amplitude and axis did not change significantly ($P>0.63$ for each, $N=5$) after delivering DC for 15000s through tube electrodes.

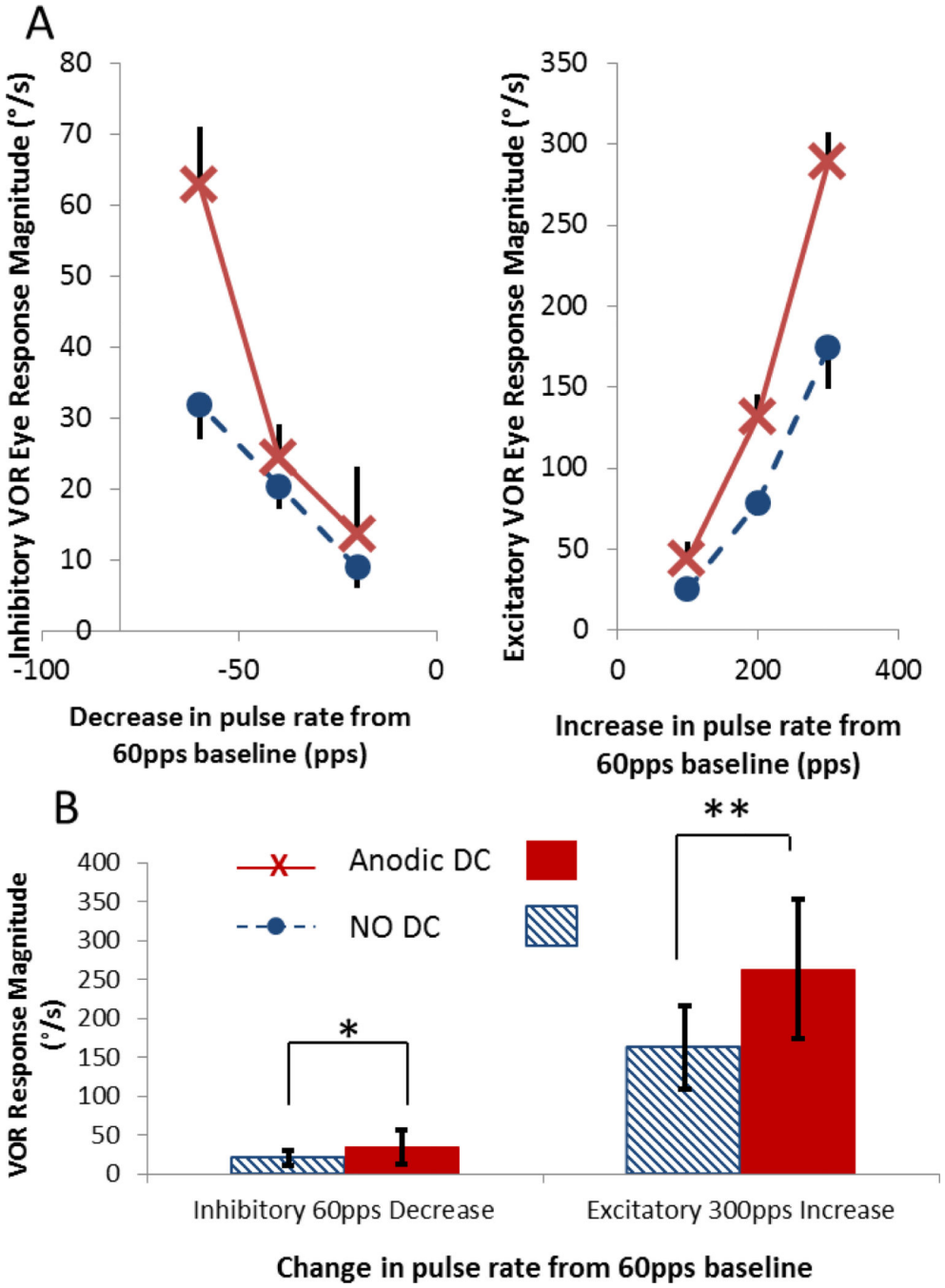

Figure 5.

VOR responses to steps in PFM when anodic DC is used to suppress the vestibular nerve are greater than for PFM alone. (A) VOR responses of chinchilla ch408 to decreasing (left plot) and increasing (right plot) steps in rate from 60pps baseline. (B) Aggregated VOR responses from all three chinchillas. Responses to the maximum decrease (right) and increase (left) in pulse rates are shown. Solid bars show VOR magnitude during combined DC and steps of PFM. Striped bars show VOR magnitude for PFM steps alone. When animals were stimulated with DC+PFM, a step decrease in pulse rate from 60pps to 0pps elicited

significantly greater inhibitory responses (*,ANOVA $F=25$, $P<0.03$), and a step increase in pulse rate from 60 pps to 300pps elicited significantly greater excitatory responses (**, ANOVA $F=334$, $P<10^{-6}$).

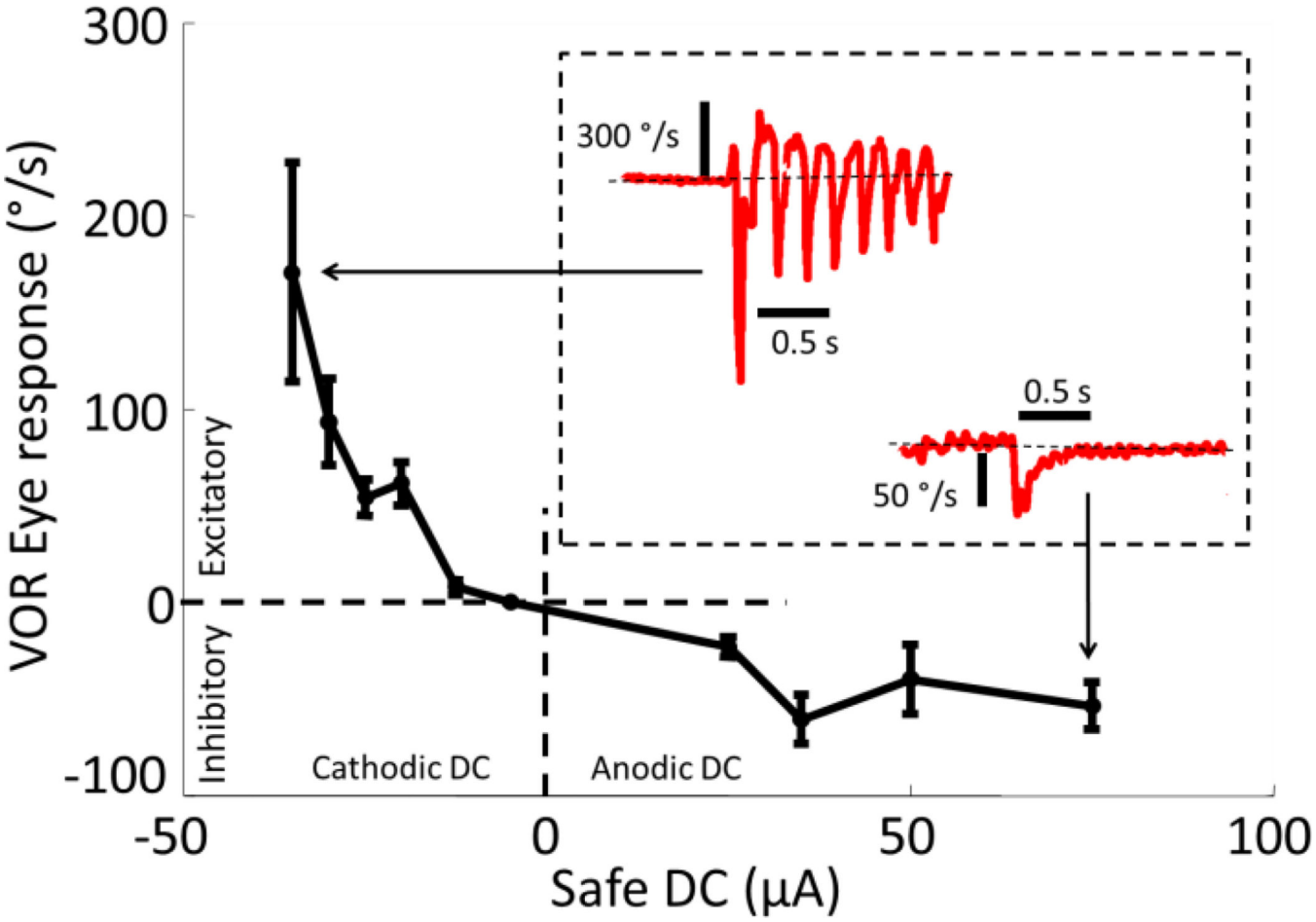

Figure 6.

VOR responses of chinchilla ch406 to steps of *safe* DC delivered using the SCDS1 stimulator connected to a perilymphatic tube electrode and distant reference in neck musculature. Positive current is anodic at the active electrode. Positive eye velocity is rightward and consistent with excitation of the implanted left labyrinth. Anodic DC evokes eye responses consistent with nerve inhibition; cathodic DC evokes responses consistent with nerve excitation. As expected, maximal inhibitory VOR responses are ~1/3 of maximal excitatory responses. Brief leftward spikes interrupting the response to cathodic DC are nystagmus quick phases, non-VOR movements that reset eye position when the eyes approach extremes of their range of motion.